*Journal of Sound and Vibration* (2000) **236**(1), 89–104
doi:10.1006/jsvi.2000.2960, available online at http://www.idealibrary.com on IDEAL®

# MEASUREMENT SELECTION FOR VIBRATION-BASED STRUCTURAL DAMAGE IDENTIFICATION

YONG XIA

*School of Civil and Structural Engineering, Nanyang Technological University, Nanyang Avenue, Singapore* 639798, *Singapore. E-mail*: *P144869448@ntu.edu.sg*

AND

HONG HAO

*School of Civil and Structural Engineering, Nanyang Technological University, Nanyang Avenue, Singapore* 639798, *Singapore. E-mail*: *chhao@ntu.eda.sg*

(*Received* 13 *October* 1999, *and in final form* 28 *January* 2000)

Many researchers have intensively investigated the methods of using vibration properties of a structure to identify its damage in the past two decades. It has been realized that the modal data included in damage identification analysis have a great influence on the accuracy of identification results. In this paper, a technique is presented to select a subset of measurement points and corresponding mode to be used in model updating for damage identification. A new concept of damage measurability is introduced in terms of two factors, namely the sensitivity of a residual vector to the structural damage, and the sensitivity of the damage to the measurement noise. Based on the two factors, the structural damage measurability is estimated quantitatively. It yields more accurate and reliable damage identification results if the mode and measurement points corresponding to the largest damage measurability value are chosen in field test and numerical analysis. The advantage of the technique is that it is based on the undamaged state of structures and thus independent of the damage configuration. Therefore, it is applicable in practice to determine the measurement selection prior to field testing and damage identification analysis. A frame structure is used to demonstrate the validity and versatility of the method. It demonstrates a significant improvement on the accuracy and reliability of damage identification results when the measurement points and mode are determined according to the present technique.


## 1. INTRODUCTION

Many structures worldwide which were constructed tens or even hundreds of years ago are still in service. Their failure could be catastrophic not only in terms of the loss in economy and life, but also in terms of the subsequent social and psychological impacts that might be caused. A lot of structures are, in fact, deficient owing to many factors such as they might not be properly designed or constructed according to modern standards, or they have been deteriorated after so many years. For example, the 1998 Report Card for America's Infrastructure pointed out that nearly 1/3–1/2 America's infrastructure (bridges, railways, school buildings, etc.) is rated structurally deficient and need to be repaired [1]. Therefore, structural condition assessment is a critical problem worldwide.

Vibration-based methods, in which the measured dynamic properties such as natural frequencies and mode shapes, are applied to detect structural damage throughout the civil,

0022-460X/00/360089 + 16 $35.00/0 

mechanical and aerospace engineering communities during the past few decades. Doebling *et al.* [2, 3] presented an intensive review of the available methods in this area. Among many techniques, finite element (FE) model updating is an attractive method, because both damage location and damage severity can be obtained by comparing the updated model with the intact model.

However, the method is far from maturing. The main difficulties lie on the two fields: uncertainties in FE modelling and errors related to modal testing [4]. Uncertainties in the FE model exist due to inaccurate physical parameters, non-ideal boundary conditions and structural non-linear properties. With respect to modal testing, measurement noise is inevitable and the maximum number of measurement locations is limited. Moreover, it is not possible till now to measure some degrees of freedom such as rotational and internal ones. Therefore, the number of equations in model updating is usually smaller than that of unknown parameters of the model, hence, it is an underdetermined problem and a small error may cause a large deviation in the results [5]. It has been realized that the locations of measurement and the modes that included in the analysis have a great influence on the accuracy of damage identification results [6, 7]. Therefore, to identify damage successfully, proper measurement selection including the measurement points and modes need to be chosen carefully before field testing and damage identification analysis.

Some methods have been developed to determine the optimal measurement set for modal test based on active vibration control theories. Lim [8] developed a method to select optimal actuator and sensor locations based on the degree of effectiveness/versatility of pairs of actuators and sensors. Kammer [9] presented a sensor placement method for modal identification and correlation according to the contribution of each candidate sensor location to the linear independence of the corresponding target modes. This algorithm was used by Klenke *et al.* [10] in developing a software environment to support optimal modal test design. Breitfeld [11] found out that the optimal set of measurement points must preserve the orthogonality of the eigenvectors to avoid spatial aliasing.

However, measurement selection for damage identification is not sufficiently studied. Sanayei and Saletnik [6] developed a Best-In-Worst-Out method to choose a subset of static force and strain measurements that have the least sensitivity to measurement noise. The available measurement which has the smallest effect on the parameter estimation is removed one by one until the output error becomes too large. Doebling *et al.* [12] studied the mode selection strategy in locating damage and concluded that a mode selection based on maximum modal strain energy produced more accurate results than that based on minimum frequency. Three mode selection techniques were examined, which are modes corresponding to the lowest modal frequency; modes that store the highest strain energy in the undamaged structure; and modes that store the highest strain energy in the damaged structure. With experimental data on an eight bay truss structure, the identification results showed that the last technique was the most effective. However, the modes in damaged structure cannot be derived in practice because the damage configuration is not available beforehand. Moreover, very high modes such as modes 105 and 106, as suggested by the results of the example, will be difficult to be measured accurately in practice.

A new technique is presented in this paper to determine the measurement set, i.e., the measurement points and the corresponding modes, for damage identification. A new concept of damage measurability is introduced in terms of two sensitivity factors, namely the sensitivity of a residual vector to the structural damage, and the sensitivity of the damage to the measurement noise. The points and mode that result in the largest damage measurability are chosen as the measurement set. This selection technique is derived from the undamaged structure and thus is independent of the damage configuration. Therefore, it can be applied to field modal testing and damage detection analysis in practice. To demonstrate the validity of the proposed method, a few example structures with different damaged members are analyzed. Without loss of generality, however, only a frame example is preserved in detail in the present paper. In numerical analysis, all the modal data are assumed containing a normally distributed variation to simulate the effect of measurement noise. Monte Carlo simulation technique is used to estimate the statistics of damage identification results. Numerical results obtained show a significant improvement on the accuracy of damage identification results when the measurement set determined by the present technique is adopted as compared with those obtained using other measurement sets.

## 2. DAMAGE MEASURABILITY

Structural damage always exists owing to many factors such as corrosion, joints loose, bumping, fatigue or improper construction. In FE model, damage can be represented by changes in some parameters such as Young's modulus, cross-sectional area, moment of inertia, and/or boundary conditions, etc. Most model updating methods modify the parameters of the model continually so that the expected responses match the measured ones in an optimal way [2]. That is, changing the parameters $\mathbf{p}$ so that the following penalty function minimizes:

$$J = \| R_m - R(\mathbf{p}) \|, \tag{1}$$

where $R(\mathbf{p})$ is a non-linear function of the parameters $\mathbf{p}$ of the structure related to the structural vibration characteristics and $R_m$ is the corresponding function obtained from measurements. Minimizing equation (1) with respect to the parameters $\mathbf{p}$, it has

$$\mathbf{S} \cdot \Delta\mathbf{p} = \mathbf{e}, \tag{2}$$

where $\mathbf{e}$ is the residual vector, $\Delta\mathbf{p}$ is the incremental vector with respect to the parameters $\mathbf{p}$ and $\mathbf{S}$ is the sensitivity matrix, which is the partial derivative of $\mathbf{e}$ with respect to $\mathbf{p}$. In general, the number of equations will not be equal to that of unknowns ($\Delta\mathbf{p}$) in equation (2). Thus usually, least-squares technique is used to solve $\Delta\mathbf{p}$. Theoretically speaking, $\Delta\mathbf{p}$ is directly related with damage. A larger value in the vector $\Delta\mathbf{p}$ corresponds to the element with a more significant damage. Thus, once $\Delta\mathbf{p}$ is determined, the damage location and level can be obtained.

The sensitivity matrix $\mathbf{S}$ represents the sensitivity of the residual vector to the changes in each parameter (i.e., damage in structures). Since a large term in $\mathbf{S}$ will cause a larger residual $\mathbf{e}$ with respect to a unit change in the parameters $\mathbf{p}$ (damage), damage will be more easily and accurately detected, thus it should be included in damage identification analysis. Specifically, in the present study, this is defined as damage sensitivity and it has

$$\mathbf{S}_d = \frac{\partial \mathbf{e}}{\partial \mathbf{p}}. \tag{3}$$

It can be obtained by estimating the change in residual vector when there is a unit change in an elemental parameter $\mathbf{p}$. $\mathbf{S}_d$ is estimated using the undamaged structural parameters because the damaged structural parameters are unknown before analysis.

The residual $\mathbf{e}$ and matrix $\mathbf{S}$ in equation (2) are also related to some uncertainties that inevitably exist in the measured data and FE model. In the present study, the effect of FE model uncertainty is not considered. The effect of measurement noise on damage identification is, however, included. It is defined as noise sensitivity and expressed as

$$\mathbf{S}_n = \frac{\partial \Delta \mathbf{p}}{\partial \mathbf{X}}, \tag{4}$$

where $\mathbf{X}$ is a noise vector. The physical meaning of $\mathbf{S}_n$ is the change in $\Delta\mathbf{p}$ due to a unit change in measurement noise and can be derived as follows. By taking partial derivative on both sides of equation (2) with respect to the measurement noise $\mathbf{X}$, it has

$$\mathbf{S}^0 \cdot \frac{\partial \boldsymbol{\Delta} \mathbf{p}}{\partial \mathbf{X}} + \frac{\partial \mathbf{S}}{\partial \mathbf{X}} \cdot \boldsymbol{\Delta} \mathbf{p}^0 = \frac{\partial \mathbf{e}}{\partial \mathbf{X}}, \tag{5}$$

where $\mathbf{S}^0$ and $\Delta\mathbf{p}^0$ are the initial values without noise. From the equation, it can be seen that the noise sensitivity, $\partial\boldsymbol{\Delta}\mathbf{p}/\partial\mathbf{X}$, is dependent on both the damage state ($\Delta\mathbf{p}^0$) and noise. Because the damage is usually unknown in practice before identification analysis, the noise sensitivity can only be approximately calculated in the undamaged state in which $\Delta\mathbf{p}^0 = \mathbf{0}$. Therefore, $\partial\boldsymbol{\Delta}\mathbf{p}/\partial\mathbf{X}$ can be approximated as

$$\frac{\partial \boldsymbol{\Delta} \mathbf{p}}{\partial \mathbf{X}} = [\mathbf{S}^u]^+ \cdot \frac{\partial \mathbf{e}}{\partial \mathbf{X}}, \tag{6}$$

where $\mathbf{S}^u$ is the sensitivity matrix in undamaged state (deterministic without noise), and superscript " + " represents the pseudo-inverse of the matrix which can be solved by singular value decomposition (SVD).

From the above definition, a large value of damage sensitivity represents that the corresponding measurement points and modes are more sensitive to structural damage; while a small value of noise sensitivity indicates that the corresponding measurement points and modes are insensitive to measurement noise. In theory, points and modes corresponding to the largest damage sensitivity and smallest nose sensitivity should be used in damage identification analysis. A large damage sensitivity assures the true damages being identifiable, and a small noise sensitivity makes the results more reliable. Both are very important and should be implemented together.

Therefore, in order to have more accurate and reliable damage identification results, one should select the measurement locations and structural modes that give the largest $\mathbf{S}_d$ and smallest $\mathbf{S}_n$. The damage measurability for a structure is thus defined as the ratio of $\mathbf{S}_d$ to $\mathbf{S}_n$

$$\mathbf{M}_d = \frac{\mathbf{S}_d}{\mathbf{S}_n}. \tag{7}$$

## 3. DAMAGE MEASURABILITY IN MODEL UPDATING METHOD WITH INCOMPLETE MODAL DATA

To apply the measurement selection method defined above to damage identification, a FE model updating method with incomplete modal data is used in this study [13]. The residual vector $\mathbf{e}$ is the modal force error function with the form

$$\mathbf{e} = -\{(\mathbf{K}_{aa} - \lambda_i \mathbf{M}_{aa}) - (\mathbf{K}_{ab} - \lambda_i \mathbf{M}_{ab})(\mathbf{K}_{bb} - \lambda_i \mathbf{M}_{bb})^{-1}(\mathbf{K}_{ba} - \lambda_i \mathbf{M}_{ba})\} \cdot \{\boldsymbol{\Phi}_a\}_i, \tag{8}$$

where $\mathbf{K}$, $\mathbf{M}$ are, respectively, the stiffness matrix and mass matrix of the undamaged structure, $\lambda_i$, $\Phi_i$ are, respectively, the $i$th measured eigenvalue and mode shape of the damaged structure. The subscripts "$a$" and "$b$" denote the measured degree of freedom (d.o.f.) and unmeasured d.o.f. respectively. Each term of $\mathbf{e}$ is the modal force error corresponding to the d.o.f. Generally, only mode shapes corresponding to the lateral d.o.f. of each point can be measured, therefore, the vector $\mathbf{e}$ has the dimension of $np \times 1$ for one mode, where $np$ is the number of measured d.o.f.s or measurement points.

First, the damage measurability of one mode is calculated. From equation (3), the damage sensitivity matrix is

$$[S_d]_{ij} = \frac{\partial \{e\}_i}{\partial \{p\}_j}, \tag{9}$$

where $i = 1, 2, \ldots, np, j = 1, 2, \ldots, ne$ in which $ne$ is the number of structural parameters to be identified, here it is the number of elements in the FE model. The $ij$th term of matrix $\mathbf{S}_d$ is the residual corresponding to the $i$th measured d.o.f. of the mode under consideration when there is a unit change in the $j$th parameter. Since damage may exist in any element, the absolute value of all the terms in the $i$th row are averaged to get the averaged sensitivity of the residual in the $i$th d.o.f. to the change of every parameter, that is

$$\{S_d\}_i = \frac{1}{ne}\sum_j |[S_d]_{ij}| = \frac{1}{ne}\sum_j \left|\frac{\partial \{e\}_i}{\partial \{p\}_j}\right|. \tag{10}$$

This is the damage sensitivity value of the $i$th d.o.f. (or $i$th measurement point). Furthermore, the damage sensitivity of the mode under consideration is the summation of the damage sensitivity values of each point, that is

$$S_d = \sum_i \{S_d\}_i. \tag{11}$$

To calculate the noise sensitivity of one mode, the source of noise must be defined first. As discussed above, the present study assumes that noise only exists in the measured modal data. Typical random measurement noise distribution has uniform or normal probability density function (PDF). A uniform PDF represents a banded type of noise with equal probability, while a normal PDF (also named as Gaussian distribution) is not banded but has a higher probability of occurrence closer to the mean value. To simulate the effect of measurement noise, the measured modal data are assumed to be the true values (without noise) plus normally distributed random noises with zero mean values and different levels of variances. That is,

$$(\lambda_i)_E = \lambda_i + \lambda_i \cdot X_{0i} = \lambda_i(1 + X_{0i}),$$

$$(\phi_{ji})_E = \phi_{ji} + \phi_{ji} \cdot X_{ji} = \phi_{ji}(1 + X_{ji}), \tag{12}$$

where $\lambda_i$ is the $i$th eigenvalue, $\phi_{ji}$ is the $j$th component of the $i$th mode shape, $i = 1, 2, \ldots, nm$, $j = 1, 2, \ldots, np$, in which $nm$ is the number of modes, subscript "$E$" represents the experimental data, $X_{0i}$, $X_{ij}$ are, respectively, the ratios of random noises in eigenvalues and mode shapes to their respective true values $\lambda_i$, $\phi_{ji}$. The mean value and variance of $X_{0i}$, $X_{ji}$ are

$$\begin{aligned} E(X_{0i}) &= 0, \qquad E(X_{ji}) = 0, \\ D(X_{0i}) &= \sigma_{0i}^2, \quad D(X_{ji}) = \sigma_{ji}^2, \end{aligned} \tag{13}$$

where $\sigma_{0i}$ and $\sigma_{ji}$ are the standard deviations, which give the level the random noise and are assumed independent of each other.

From equation (4), the noise sensitivity matrix of one mode is

$$[S_n]_{ij} = \frac{\partial \{\Delta p/p\}_j}{\partial X_i}. \tag{14}$$

Here the parameter change ratio (damage ratio) $\Delta \mathbf{p}/\mathbf{p}$ is used instead of $\Delta \mathbf{p}$. It indicates no damage in the particular element if its damage ratio is equal to zero; and total loss of the elemental stiffness if its damage ratio equals $-1$. The matrix $\mathbf{S}_n$ also has dimensions $np \times ne$. The $ij$th term of the matrix $S_n$ is the change in the $j$th elemental damage ratio when there is a unit change (noise) in the measured data at the $i$th d.o.f. If the noise in the eigenvalue of the mode is also considered, the noise sensitivity matrix has the dimension of $(np+1)\times ne$. In that case the $j$th component of row $(np+1)$ is the change in the $j$th elemental damage ratio when there is a unit change (noise) in the measured eigenvalue of the mode. Similar to equation (10), the absolute values of all the terms in the $i$th row are averaged to obtain the noise sensitivity value of $i$th d.o.f., which means the averaged influence of noise in the measured data at the $i$th d.o.f. on the elemental damage ratio, it has

$$\{S_n\}_i = \frac{1}{ne}\sum_j |[S_n]_{ij}| = \frac{1}{ne}\sum_j \left|\frac{\partial \{\Delta p/p\}_j}{\partial X_i}\right|. \tag{15}$$

Furthermore, the noise sensitivity of the mode under consideration is the summation of the noise sensitivity value of each d.o.f. (point). It has

$$S_n = \sum_i \{S_n\}_i. \tag{16}$$

According to the properties of damage sensitivity and noise sensitivity, the damage measurability of one point is defined as the ratio of the damage sensitivity to the noise sensitivity of that point,

$$\{M_d\}_i = \frac{\{S_d\}_i}{\{S_n\}_i} \tag{17}$$

and the damage measurability of a mode is similarly defined as the ratio of the damage sensitivity to the noise sensitivity of that mode

$$M_d = \frac{S_d}{S_n} = \frac{\sum_i \{S_d\}_i}{\sum_i \{S_n\}_i}. \tag{18}$$

The above procedure can be repeated for each mode of interest, thus the damage measurability of each point in the first few modes can be derived before field measurement and damage identification analysis. The mode with the largest damage measurability is chosen and the points with larger damage measurability corresponding to the chosen mode are selected as measurement d.o.f.s.

## 4. NUMERICAL EXAMPLE

The above procedures have been used to analyze several examples. Without loss of generality, however, only one frame example is presented in detail in this section to demonstrate the validity of the method. First, the damage measurability of the structure is calculated, from this the measurement selection is derived; then, the assumed damages are introduced and identified by model updating method. To study the effect of measurement noise, each eigenvalue and mode shape are assumed having some random variations as described above. Monte Carlo simulation is employed to estimate the statistics of identification results obtained with or without using the optimal measurement sets.

Consider a two-level, one span concrete frame structure as shown in Figure 1. Table 1 gives its mechanical parameters. The frame is discretized into 32 beam-column elements with 32 nodes. Each element has 6 d.o.f.s, besides the mass of the frame, non-structural mass of 3000 kg/m is also added to the beams in finite element modelling.

Damage is defined as the reduction of elemental flexural stiffness. The parameter **p** represents the elemental flexural stiffness ($EI$) and damage ratio $\Delta\mathbf{p}/\mathbf{p}$ thus represents elemental stiffness change ratio. Since only transverse response can be measured in practice, dynamic characteristics corresponding to the lateral d.o.f.s at 30 nodes are assumed to be measured. Therefore, *np*, *ne* are 30 and 32 respectively.

The damage sensitivity is estimated for each point according to equation (10) and summed up for one mode as equation (11). The results for the first 7 modes are listed in

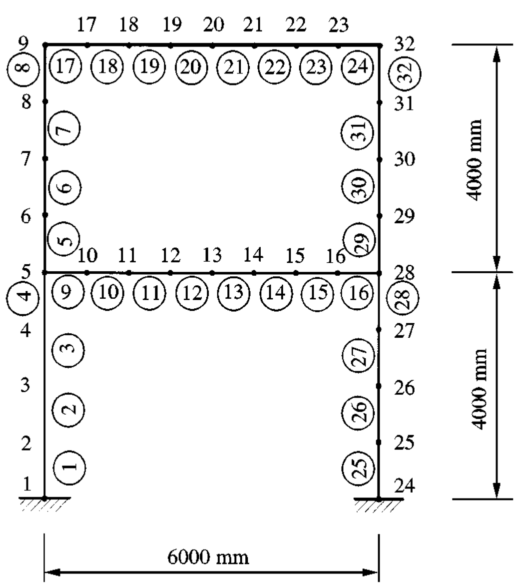


Figure 1. Finite element model of frame.

Table 1

*Nominal properties of structure*

| | Area A ($m^2$) | Density $\rho$ ($kg/m^3$) | Young's modulus E ($N/m^2$) | Moment of inertia I ($m^4$) | Axial stiffness $EA$ (N) | Linear density $\bar{m}$ (kg/m) | Flexural stiffness $EI$ ($N\,m^2$) |
|---|---|---|---|---|---|---|---|
| Column | $0{\cdot}4 \times 0{\cdot}4$ | $2{\cdot}50 \times 10^3$ | $2{\cdot}50 \times 10^{10}$ | $2{\cdot}1 \times 10^{-3}$ | $4{\cdot}00 \times 10^9$ | $4{\cdot}00 \times 10^3$ | $5{\cdot}33 \times 10^7$ |
| Beam | $0{\cdot}25 \times 0{\cdot}5$ | $2{\cdot}50 \times 10^3$ | $2{\cdot}50 \times 10^{10}$ | $2{\cdot}6 \times 10^{-3}$ | $3{\cdot}13 \times 10^9$ | $3{\cdot}31 \times 10^3$ | $6{\cdot}51 \times 10^7$ |

Table 2. Similarly, the noise sensitivity is estimated for each point according to equation (15) and summed up for one mode as equation (16). The results for the first 7 modes are listed in Table 3. It should be noted that the symmetric points have the same values. The noise sensitivity of points 13 and 20 for some modes are zero because they are the stationary nodes of those modes. Thus, the corresponding mode shape values are zero.

TABLE 2

*Damage sensitivity matrix* ($S_d$) ($\times 10^6$)

| Points | Mode 1 | Mode 2 | Mode 3 | Mode 4 | Mode 5 | Mode 6 | Mode 7 |
|---|---|---|---|---|---|---|---|
| 2, 25 | 0·0817 | 0·2478 | 0·1093 | 0·2249 | 0·1486 | 0·4609 | 0·0301 |
| 3, 26 | 0·0669 | 0·2172 | 0·1253 | 0·2829 | 0·1857 | 0·5097 | 0·0901 |
| 4, 27 | 0·0915 | 0·2574 | 0·1665 | 0·4740 | 0·3507 | 0·7038 | 0·3023 |
| 5, 28 | 0·0736 | 0·4508 | 0·2558 | 0·5354 | 0·3853 | 0·8522 | 0·3385 |
| 6, 29 | 0·0780 | 0·2533 | 0·2904 | 0·4513 | 0·4835 | 0·7716 | 0·4463 |
| 7, 30 | 0·0614 | 0·2511 | 0·3707 | 0·3302 | 0·5569 | 0·5561 | 0·5499 |
| 8, 31 | 0·0710 | 0·2455 | 0·4507 | 0·2764 | 0·6133 | 0·4464 | 0·8577 |
| 9, 32 | 0·0440 | 0·1454 | 0·2251 | 0·1592 | 0·2704 | 0·2989 | 0·5448 |
| 10, 16 | 0·1623 | 0·3401 | 0·3552 | 0·8763 | 0·8019 | 1·8362 | 1·4513 |
| 11, 15 | 0·1653 | 0·0971 | 0·3691 | 1·0887 | 0·4712 | 2·7351 | 1·5225 |
| 12, 14 | 0·1107 | 0·0400 | 0·4246 | 1·3372 | 0·2222 | 2·8363 | 1·4451 |
| 17, 23 | 0·1110 | 0·3902 | 0·5943 | 0·4585 | 1·5646 | 0·7576 | 1·8340 |
| 18, 22 | 0·1116 | 0·4272 | 0·9081 | 0·4313 | 2·7464 | 0·5799 | 3·7122 |
| 19, 21 | 0·0693 | 0·2779 | 1·1822 | 0·4271 | 2·7012 | 0·2900 | 3·7222 |
| 13 | 0·0885 | 0·0264 | 0·4603 | 1·5017 | 0·1560 | 2·4959 | 1·4586 |
| 20 | 0·0540 | 0·2194 | 1·3106 | 0·4629 | 2·3491 | 0·2079 | 3·7260 |
| $\Sigma$ | 2·7391 | 7·5278 | 13·4255 | 16·6714 | 25·5089 | 29·9732 | 38·8786 |

TABLE 3

*Noise sensitivity matrix* ($S_n$)

| Points | Mode 1 | Mode 2 | Mode 3 | Mode 4 | Mode 5 | Mode 6 | Mode 7 |
|---|---|---|---|---|---|---|---|
| 2, 25 | 0·2475 | 0·5856 | 0·3352 | 0·3382 | 0·3597 | 0·3764 | 0·0799 |
| 3, 26 | 2·2319 | 3·7727 | 0·7436 | 0·7661 | 0·8911 | 0·8003 | 0·2500 |
| 4, 27 | 8·6009 | 11·6446 | 0·8119 | 1·4074 | 1·4106 | 0·8916 | 0·7504 |
| 5, 28 | 131·1439 | 228·6121 | 0·5693 | 0·1038 | 3·6295 | 0·5455 | 13·4540 |
| 6, 29 | 21·1453 | 33·4981 | 1·1026 | 1·2830 | 1·3066 | 0·6233 | 5·9619 |
| 7, 30 | 20·5836 | 6·2853 | 0·9836 | 0·5914 | 1·0996 | 1·6793 | 0·6333 |
| 8, 31 | 38·8181 | 4·2970 | 0·4475 | 0·1480 | 0·5034 | 1·4497 | 0·6456 |
| 9, 32 | 372·1350 | 160·4135 | 0·0664 | 0·2254 | 0·0670 | 1·8105 | 0·2335 |
| 10, 16 | 9·0648 | 2·8390 | 3·9716 | 4·4687 | 3·6881 | 1·7127 | 1·1781 |
| 11, 15 | 1·7802 | 1·0248 | 4·1383 | 4·9259 | 0·1027 | 1·8092 | 3·3617 |
| 12, 14 | 1·8363 | 1·2417 | 3·0985 | 3·2839 | 0·3703 | 1·2587 | 0·3974 |
| 17, 23 | 2·6042 | 5·7020 | 4·5822 | 2·2586 | 1·8010 | 1·0446 | 2·5216 |
| 18, 22 | 1·3065 | 1·7413 | 4·6805 | 4·9889 | 2·0149 | 0·1367 | 0·4949 |
| 19, 21 | 1·4374 | 1·5552 | 3·3876 | 3·0543 | 1·2321 | 0·3662 | 0·4101 |
| 13 | 0 | 0 | 2·8062 | 3·6172 | 0 | 0 | 0·9231 |
| 20 | 0 | 0 | 2·9437 | 3·2997 | 0 | 0 | 0·9188 |
| $\Sigma$ | 1225·871 | 926·4258 | 63·5875 | 62·6041 | 36·9532 | 29·0094 | 62·5867 |
| Eigenvalue | 0·0499 | 0·1953 | 0·2273 | 0·2610 | 0·5269 | 0·3694 | 2·0092 |

TABLE 4

*Damage measurability of the first seven modes* ($M_d$)

| | Mode 1 | Mode 2 | Mode 3 | Mode 4 | Mode 5 | Mode 6 | Mode 7 |
|---|---|---|---|---|---|---|---|
| $S_d(\times 10^6)$ | 2·7391 | 7·5278 | 13·4255 | 16·6714 | 25·5089 | 29·9732 | 38·8786 |
| $S_n$ | 1225·871 | 926·4258 | 63·5875 | 62·6041 | 36·9532 | 29·0094 | 62·5867 |
| $M_d(\times 10^6)$ | 0·0022 | 0·0081 | 0·2111 | 0·2663 | 0·6903 | 1·0332 | 0·6212 |

From the results obtained, it can be noted that the damage sensitivity value for each mode increases with the mode number. This is because, as commonly understood, higher modes will be more sensitive to damage, especially the localized damage. On the other hand, the noise sensitivity values of the first mode and the second mode are very large, therefore it will render significant error if they are included in damage identification analysis. The noise sensitivity value generally decreases with the increase of the mode number, but the decrease is not monotonic. As given in Table 3, the noise sensitivity of mode 7 is larger than that of modes 5 and 6. A detailed mode shape analysis indicates that there is a large axial deformation associated with mode 7. This is probably the reason that the noise sensitivity of mode 7 is larger. In fact, noise sensitivity values of higher modes, which are not given here, are also calculated. It is found that the noise sensitivity value of mode 9 is the smallest in the first 9 modes. Although it is possible but very difficult and expensive to measure the high modes accurately in practice, the lower modes that give relatively small noise sensitivity should be chosen in practice. Without loss of generality, in the present example, only the first 7 modes are considered.

From equation (18), the damage measurability of each mode is estimated and listed in Table 4.

It can be seen clearly in Table 4 that mode 6 is the most suitable one among the first 7 modes for damage identification analysis. Moreover, the sixth mode also corresponds to a smaller noise sensitivity to eigenvalue than the fifth and the seventh mode (see Table 3). Therefore, mode 6 is chosen in the analysis.

To search for the proper points, the damage measurability of the lateral d.o.f. of each point is estimated according to equation (17). The results are given in Table 5. Points 13 and 20 are excluded because they are the stationary nodes of mode 6. From Table 5, the 12 points which have relatively larger damage measurability values are selected as measurement points, they are: Nos. 2, 5, 6, 11, 12, 18 and the symmetric ones (Nos. 25, 28, 29, 15, 14, 22).

It should be noted that the above procedure is performed based on the finite element model of the intact structure. It does not pre-assume the locations and damage levels in the structure. This implies the versatility of the method that it can be applied to any structure with any damage state before damage identification analysis. The chosen mode and measurement points vary from structure to structure depending on structural parameters, configurations and the number of modes considered. Moreover, how many points are included in the measurement and analysis depend on the availability of measurement equipment, and experience of the analyst. More points do not mean better results because more measurement errors are introduced.

To illustrate the advantage of the measurement selection based on the presented algorithm in structural damage identification, two damaged states and three sets of measurement selections are considered. The detail information is listed in Table 6. In the first damage state, elements 1–4 (the left column in the first storey) are assumed deteriorated

TABLE 5

*Damage measurability of measurement points in mode 6 ($M_d$)*

| Points (1) | $S_d(\times 10^6)$ (2) | $S_n$ (3) | $M_d$ $(\times 10^6)$ (4) = (2)/(3) |
|---|---|---|---|
| 2, 25 | 0·4609 | 0·3764 | **1·2245** |
| 3, 26 | 0·5097 | 0·8003 | 0·6369 |
| 4, 27 | 0·7038 | 0·8916 | 0·7894 |
| 5, 28 | 0·8522 | 0·5455 | **1·5622** |
| 6, 29 | 0·7716 | 0·6233 | **1·2379** |
| 7, 30 | 0·5561 | 1·6793 | 0·3311 |
| 8, 31 | 0·4464 | 1·4497 | 0·3079 |
| 9, 32 | 0·2989 | 1·8105 | 0·1651 |
| 10, 16 | 1·8362 | 1·7127 | 1·0721 |
| 11, 15 | 2·7351 | 1·8092 | **1·5118** |
| 12, 14 | 2·8363 | 1·2587 | **2·2534** |
| 17, 23 | 0·7576 | 1·0446 | 0·7253 |
| 18, 22 | 0·5799 | 0·1367 | **4·2421** |
| 19, 21 | 0·2900 | 0·3662 | 0·7919 |

TABLE 6

*Detail of damage cases and measurement selections*

| Case | Damage state | Damaged elements (damage ratios) | Measurement selection | Mode/measurement points |
|---|---|---|---|---|
| 1 | 1 | 1, 2, 3, 4 (– 15·5%) | 1 | Mode 6/2, 5, 6, 11, 12, 14, 15, 18, 22, 25, 28, 29 |
| 2 | | | 2 | Mode 6/3, 5, 7, 9, 11 13, 15, 18, 20, 22, 26, 28, 30, 32 |
| 3 | | | 3 | Mode 5/2, 5, 6, 11, 12, 14, 15, 18, 22, 25, 28, 29 |
| 4 | 2 | 1, 11, 21, 30 (– 15·5%) | 1 | Mode 6/2, 5, 6, 11, 12, 14, 15, 18, 22, 25, 28, 29 |
| 5 | | | 2 | Mode 6/3, 5, 7, 9, 11, 13, 15, 18, 20, 22, 26, 28, 30, 32 |
| 6 | | | 3 | Mode 5/2, 5, 6, 11, 12, 14, 15, 18, 22, 25, 28, 29 |

with a flexural stiffness reduction by 15·5%. In the second state, damage is assumed existing in arbitrarily selected elements. In particular, elements 1, 11, 21 and 30 have flexural stiffness reduction by 15·5%. The first measurement selection is the above chosen measurement set; the second selection is the measurement at alternative points of mode 6; and the last one is the same measurement points as the first selection but mode 5 is used in the analysis.

In different cases, only the lateral d.o.f.s of the selected points are measured and the damage is identified by the model updating method. To consider the influence of measurement noise, the simulated modal data are set to be the true values smeared with random noises, which are assumed having normal distributions, as given in equations (12) and (13). Monte Carlo simulation is used to estimate the statistics of damage ratios of the structure. The procedure is summarized in the following:

1. add Gaussian random noise with zero mean and prescribed standard deviation to the true modal data;
2. identify the damages with model updating method and calculate the damage ratios of all elements;
3. repeat steps 1 and 2, then compute the means and standard deviations of damage ratios for all elements;
4. stop simulations until the means and standard deviations converge;
5. repeat steps 1–4 for each case and compare their results.

The noise is assumed having a standard deviation of 0·5% for eigenvalue and 1·0% for every mode shape amplitude. That is $\sigma_{0i} = 0{\cdot}5\%$ and $\sigma_{ji} = 1{\cdot}0\%$, $j = 1, 2, \ldots, np$. According to the above procedures, the results of Cases 1–3 are derived and illustrated in Figures 2–5.

Figure 2 compares the mean values of damage ratios obtained from Cases 1 and 2 with the true damage ratios (− 15·5%). It can be seen that in Cases 1 and 2, the damage ratios of damaged elements are approximately equal to the true values except that of element 2. But Case 1 has smaller errors in the undamaged elements (Nos. 5–32), where the true damage values are zero. Damage in element 2 is not detected because the element stores small modal strain energy associated with mode 6, thus the damage in this element produces negligible changes in the dynamic characteristics of the mode so that the damage cannot be identified. Similar observations that this certain mode is insensitive to damage in particular elements were also made by other researchers [14]. To overcome this problem, multiple modes should be included in the analysis. This, however, is not a topic of the present paper.

Figure 3 compares the standard deviations of damage ratios obtained in Cases 1 and 2. It shows that the standard deviations of nearly all elemental damage ratios of Case 1 are much smaller than those of Case 2, which means the damages can be identified more reliably in

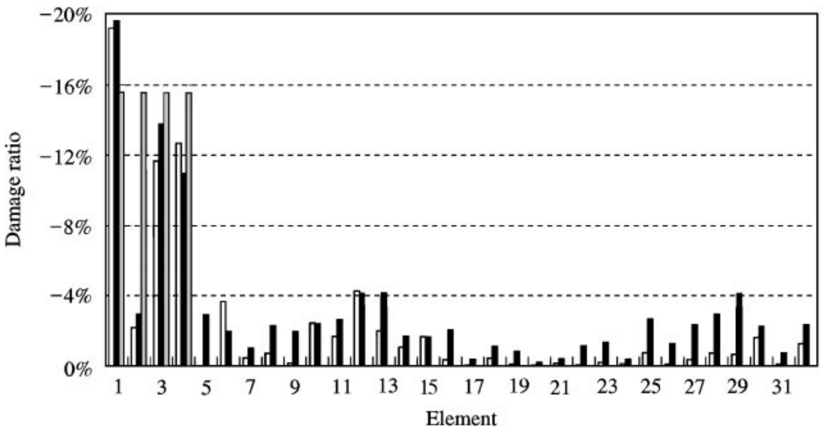


Figure 2. Mean values of Case 1 versus Case 2: □, Case 1; ■, Case 2; ▤, True value.

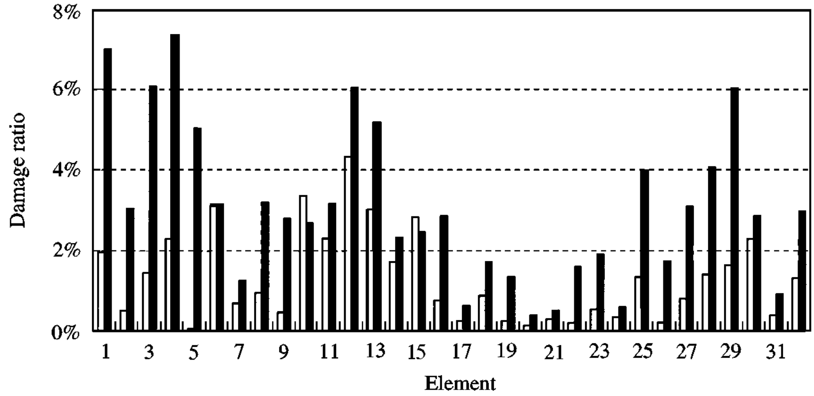


Figure 3. Standard deviations of Case 1 versus Case 2: □, Case 1; ■, Case 2.

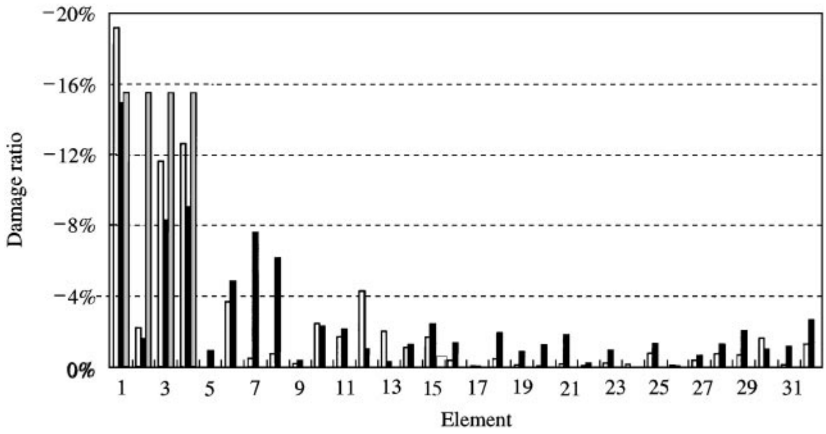


Figure 4. Mean values of Case 1 versus Case 3: □, Case 1; ■, Case 3; ▤, True value.

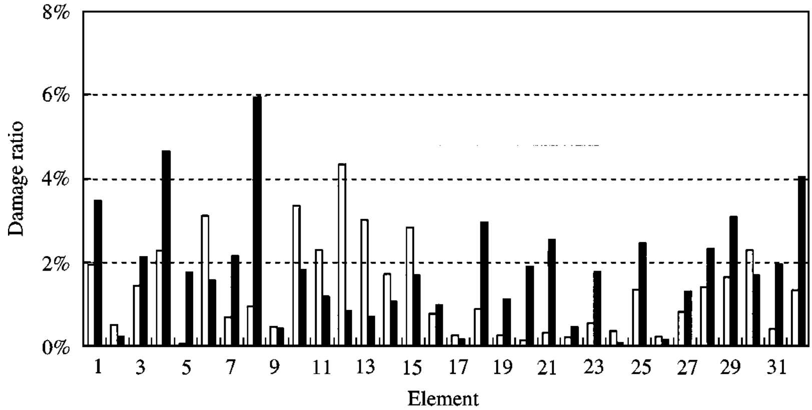


Figure 5. Standard deviations of Case 1 versus Case 3: □, Case 1; ■, Case 3.

Case 1 than in Case 2. These observations indicate that using the proper measurement points determined by the damage measurability analysis introduced in this paper can improve the accuracy and reliability of damage identification results.

Similarly, Figures 4 and 5 compare the mean values and standard deviations of Case 1 with those of Case 3 respectively. It shows that damage in element 2 cannot be identified in Case 3 either, implying mode 5 is not sensitive to the damage in element 2 either. Case 3 also results in larger errors in damage ratios of the damaged elements 3, 4, and results in false damage locations in undamaged elements 7, 8. Moreover, Case 3 generally has larger standard deviations of damage ratios as compared with those of Case 1. These observations indicate that using proper mode determined by damage measurability analysis can improve the accuracy and reliability of identification results.

To check the general applicability of the proper selection to different damage configurations, a more general damage state (damage state 2) is examined in which the damaged elements are selected arbitrarily rather than concentrated in one column. Figures 6–9 show the results.

As shown, both Cases 4 and 5 can detect damage in elements 1, 11 and 30, but fail to detect damage in element 21. Case 5 gives false damage detection in a few elements such as 3, 4, 5 and 31. Moreover, Case 5 also results in larger standard deviations in almost all elements than Case 4 does, implying the identification results of Case 4 are more reliable. Both cases fail to detect damage in element 21 is because of the same reason as discussed above for element 2. Nevertheless, identification results shown in Figures 6 and 7 demonstrated again that using the measurement set proposed in this study can give more accurate and more reliable damage detection results.

If mode 5 is used instead of mode 6, as shown clearly in Figures 8 and 9, the damages in elements 11, 21 and 30 are not detected. This demonstrates again the advantages of using the proper measurement selection in the analysis, although the averaged standard deviations in Case 6 are comparable to those in Case 4.

The average errors of the mean values and the average standard deviations of the six cases analyzed above are estimated by

$$\text{Average error of mean values } \bar{e}_\mu = \frac{\sum_{i=1}^{ne} |\mu(\alpha_i^S) - \alpha_i^T|}{ne}, \tag{19}$$

$$\text{Average standard deviations } \bar{e}_\sigma = \frac{\sum_{i=1}^{ne} \sigma(\alpha_i^S)}{ne}, \tag{20}$$

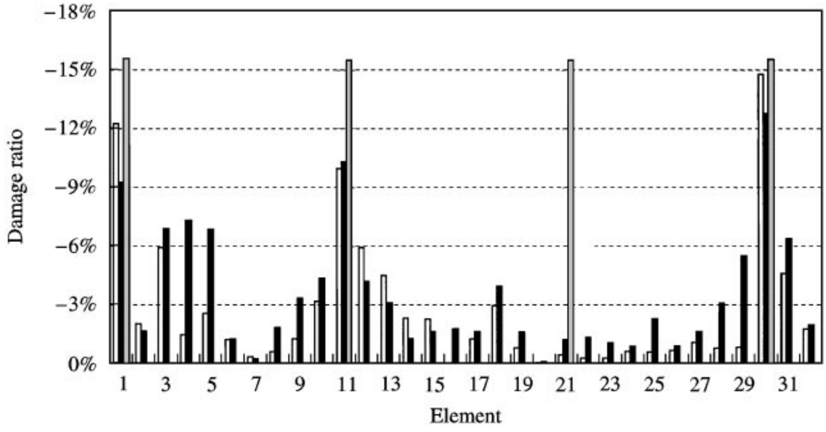


Figure 6. Mean values of Case 4 versus Case 5: □, Case 4; ■, Case 5; ▤, True value.

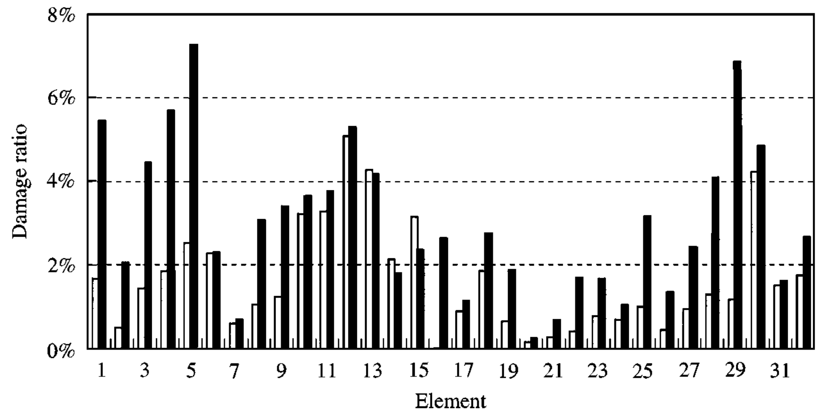


Figure 7. Standard deviations of Case 4 versus Case 5: □, Case 4; ■, Case 5.

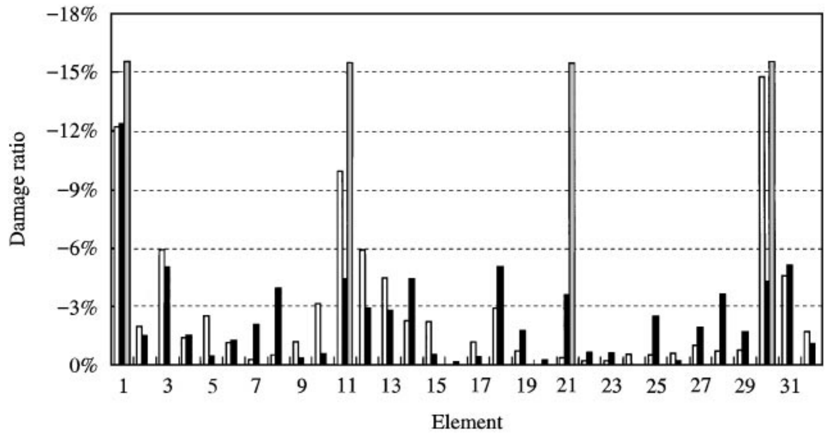


Figure 8. Mean values of Case 4 versus Case 6: □, Case 4; ■, Case 6; ▤, True value.

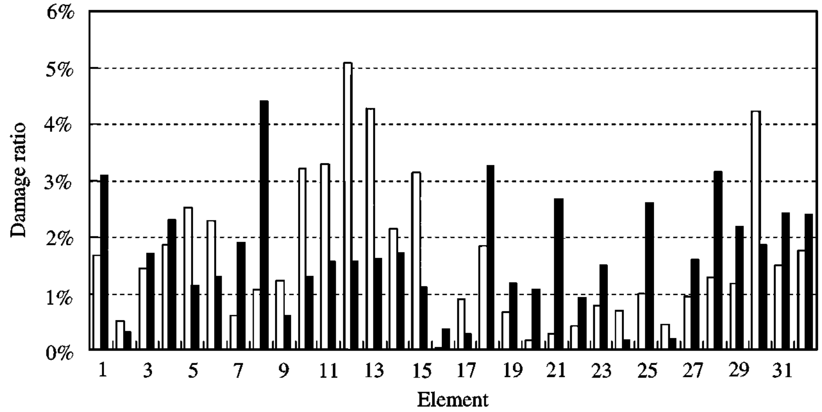


Figure 9. Standard deviations of Case 4 versus Case 6: □, Case 4; ■, Case 6.

TABLE 7

*Average errors of mean values ($\bar{e}_\mu$) and avearge standard deviations ($\bar{e}_\sigma$)*

| | Case 1 | Case 2 | Case 3 | Case 4 | Case 5 | Case 6 |
|---|---|---|---|---|---|---|
| $\bar{e}_\mu$ | 0·0158 | 0·0244 | 0·0242 | 0·0234 | 0·0333 | 0·0285 |
| $\bar{e}_\sigma$ | 0·0135 | 0·0310 | 0·0186 | 0·0165 | 0·0302 | 0·0168 |

where $\mu$, $\sigma$ are, respectively, the mean value and standard deviation, $\alpha_i^S$ is the simulated results of damage ratio of element *i* and $\alpha_i^T$ is the true damage ratio of element *i*. Table 7 lists the results. As can be noted, identification results obtained by using the proper selection (Cases 1 and 4) give more accurate (smaller average error) and more reliable (smaller average standard deviation) damage detection.

Therefore, with the proper measurement points and mode derived by this technique, most damaged elements can be identified more accurately and reliably, although a few damaged elements might not be detected. Results might be improved if multiple modes are used in the analysis, and this will be a subject of further study in the future. It should be noted that there is no proof of the selected measurement set being absolutely optimal among all permutations of measurement points. Nevertheless, the above results demonstrated that using the measurement points and mode determined from damage measurability analysis, damage identification results will be more accurate and reliable as compared with those obtained by using other measurement points and mode in the analysis.

To investigate the general applicability of the method, a few other examples with different structural configurations were also examined. They all demonstrate that with proper selection of measurement points and mode, more accurate and reliable results will be derived. Nevertheless, these examples are not included in the present paper purely for concise consideration.

## 5. CONCLUSIONS

A method has been developed and presented in this paper to derive a proper set of measurement points and mode to be used in FE model updating analysis for structural damage identification. It is based on the damage measurability of a structure defined in terms of damage sensitivity and noise sensitivity. Before detecting damage, damage measurability analysis of the structural model is performed. The mode with the largest damage measurability among all the available modes, and the points with the largest damage measurability corresponding to that mode should be selected in measurement and damage analysis. This selecting set has the maximum sensitivity to structural damage and minimum sensitivity to measurement noise.

The presented algorithm is based on the FE model in undamaged state and is independent of damage configuration. Thus, it can be applied to any structure with any damage state prior to field modal testing and damage identification analysis.

The proposed procedure has been applied to identify damages in example structures. Numerical results have demonstrated the improvement on both accuracy and reliability of the damage identification results.

## REFERENCES

1. *ASCE News* 1998 **23**. The 1998 Report Card for America's infrastructure.

2. S. W. Doebling, C. R. Farrar, M. B. Prime and D. W. Shevitz 1996 *Los Alamos National Laboratory Report LA*-13070-*MS*. Damage identification and health monitoring of structural and mechanical systems from changes in their vibration characteristics: a literature review.
3. S. W. Doebling, C. E. Farrar and M. B. Prime 1998 *The Shock and Vibration Digest* **30**, 91–105. A summary review of vibration-based damage identification methods.
4. M. I. Friswell, J. E. T. Penny and S. D. Garvey 1997 *Inverse Problems in Engineering* **5**, 189–215. Parameter subset selection in damage location.
5. J. H. Wang and C. M. Liou 1991 *Journal of Vibration and Sound*, *Transaction of the ASME* **113**, 28–36. Experimental identification of mechanical joint parameters.
6. M. Sanayei and M. J. Saletnik 1996 *ASCE Journal of Structural Engineering* **122**, 563–572. Parameter estimation of structures from static strain measurements Part II: error sensitivity analysis.
7. B. Gunes, B. Arya, S. Wadia-Fascetti and M. Sanayei 1999 *Computational Mechanics in Structural Engineering*: *Recent Developments* (F. Cheng and Y. Gu, editors) 193–206. Amsterdam: Elsevier Scientific Ltd. Practical issues in the application of structural identification.
8. K. B. Lim 1992 *Journal of Guidance*, *Control*, *and Dynamics* **15** 49–57. Method for optimal actuator and sensor placement for large flexible structures.
9. D. C. Kammer 1991 *Journal of Guidance*, *Control*, *and Dynamics* **14**, 251–259. Sensor placement for on-orbit modal identification and correlation of large space structures.
10. S. E. Klenke G. M. Reese, L. A. Schoof and C. Shierling 1995 *Matlab Conference*, *http://endo.sandia.gov/*9234*/papers/veto/matlab.html*. Modal test optimization using VETO (virtual environment for test optimization).
11. T. Breitfeld 1996 *Modal Analysis*: *The International Journal of Analytical and Experimental Modal Analysis* **11**, 1–9. A method for identification of a set of optimal measurement points for experimental modal analysis.
12. S. W. Doebling, F. M. Hemez L. D. Peterson and C. Farhat 1997 *AIAA Journal* **35**, 693–699. Improved damage location accuracy using strain energy-based mode selection criteria.
13. M. Sanayei, S. Wadia-Fascetti, J. A. S. McClain, I. Gornshteyn and E. M. Santini 1998 *Proceedings of the Structural Engineers World Congress*. Structural parameter estimation using modal responses and incorporating boundary conditions.
14. T. W. Lim 1991 *AIAA Journal* **29**, 2271–2274. Structural damage detection using modal test data.